View metadata, citation and similar papers at core.ac.uk

brought to you by CORE

provided by Kyoto University Research Information Repository

KURENAI
Kyoto University Research Information Repository

KYOTO UNIVERSITY

| | |
|---|---|
| Title | Rutherford Backscattering Spectrometry Analysis of Self-Formed Ti-Rich Interface Layer Growth in Cu(Ti)/Low-k Samples |
| Author(s) | Kohama, Kazuyuki; Ito, Kazuhiro; Mori, Kenichi; Maekawa, Kazuyoshi; Shirai, Yasuharu; Murakami, Masanori |
| Citation | Journal of Electronic Materials (2009), 38(9): 1913-1920 |
| Issue Date | 2009-09 |
| URL | http://hdl.handle.net/2433/126666 |
| Right | The original publication is available at www.springerlink.com |
| Type | Journal Article |
| Textversion | author |

Kyoto University

# Rutherford Backscattering Spectrometry Analysis of Self-Formed Ti-Rich Interface Layer Growth in Cu(Ti)/Low-k Samples

Kazuyuki Kohama,[1] Kazuhiro Ito,[1] Kenichi Mori,[2] Kazuyoshi Maekawa,[2] Yasuharu Shirai[1] and Masanori Murakami[3]

1. *Department of Materials Science and Engineering, Kyoto University, Kyoto 606-8501, Japan*
2. *Process Technology Development Division, Renesas Technology Corporation, Itami, Hyogo 664-0005, Japan*
3. *The Ritsumeikan Trust, Nakagyo-ku, Kyoto 604-8520, Japan*

Corresponding Author : Kazuhiro ITO

E-mail: kazuhiro-ito@mtl.kyoto-u.ac.jp

Tel: +81-75-753-5472 / Fax: +81-75-753-3579

ABSTRACT

A new fabrication technique to prepare ultra-thin barrier layers for nano-scale Cu wires was proposed in our previous studies. Ti-rich layers formed at Cu(Ti)/dielectric-layer interfaces consisted of crystalline TiC or TiSi and amorphous Ti oxides. The primary control factor for the Ti-rich interface layer composition was C concentration in the dielectric layers rather than the formation enthalpy of the Ti compounds. To investigate Ti-rich interface layer growth in Cu(Ti)/dielectric-layer samples annealed in ultra high vacuum, Rutherford backscattering spectrometry (RBS) was employed in the present study. Ti peaks were obtained only at the interfaces for all samples. Molar amounts of Ti atoms segregated to the interfaces ($n$) were estimated from Ti peak areas. Log $n$ values were proportional to log $t$ values. Slopes were similar for all samples, suggesting similar growth mechanisms. The activation energy ($E$) for Ti atoms reacting with the dielectric layers containing carbon (except $SiO_2$) tended to decrease with decreasing C concentration (decreasing $k$), while those for the $SiO_2$ layers were much higher. Reaction rate coefficients ($Z \cdot \exp(-E/RT)$) were insensitive to C concentration in the dielectric layers. These factors lead to the conclusion that growth of the Ti-rich interface layers is controlled by chemical reactions, represented by the $Z$ and $E$ values, of the Ti atoms with the dielectric layers, although there are a few diffusion processes possible.

**Key words**: Cu(Ti) alloy film, low-k films, self-formation, Rutherford backscattering spectrometry, diffusion barrier

## INTRODUCTION

In our previous studies, a new fabrication technique to prepare ultra-thin barrier layers for nano-scale Cu wires was proposed. Supersaturated Cu(Ti) alloy films deposited on dielectric layers such as $SiO_2$ and $SiO_xC_y$ with low dielectric constants (low-k) were annealed at elevated temperatures, and thin Ti-rich layers were found to be formed at the interfaces.[1,2] The Ti-rich layers formed at the interfaces were found to consist of crystalline TiC or TiSi in addition to amorphous Ti oxides. The primary factor to control composition of the self-formed Ti-rich interface layers was the C concentration in the dielectric layers rather than the formation enthalpy of the Ti compounds (TiC and TiSi). Crystalline TiC was formed on the dielectric layers with a C concentration higher than 17 at.%. [2]

Transmission electron microscopy (TEM) observation and electrical resistivity measurements indicated that growth of the Ti-rich interface layers consisting of TiC (Cu(1 at.%Ti)/low-k samples) was faster than those consisting of TiSi (Cu(1at.%Ti)/$SiO_2$ samples) after annealing at 400°C.[3] For systematic investigation of dependence of initial Ti contents in the Cu(Ti) alloy films and C concentrations in the dielectric layers on the Ti-rich interface layer growth, the Rutherford backscattering spectrometry (RBS) technique was employed instead of TEM in the present studies.

## EXPERIMENTAL PROCEDURES

The Cu(1, 5, and 10 at.%Ti) alloy films were deposited on $SiO_xC_y$ (low-k1 and low-k4), $SiO_2$, SiCO, and SiCN dielectric layers by a radio frequency magnetron sputtering technique. The low-k1, low-k4, SiCO, and SiCN dielectric layers were grown on (100)-oriented Si wafers using conventional plasma chemical vapor deposition

methods. The $SiO_2$ layer was grown on the Si substrate by oxidation. The dielectric constants ($k$) and compositions of these layers are shown in Table 1. Prior to film deposition, the substrates were ultrasonically cleaned with acetone and isopropyl alcohol. The base pressure prior to deposition was approximately $1 \times 10^{-6}$ Pa, and the sputtering power and working pressure were kept at 300 W and about 1 Pa, respectively. The substrate holder was placed 100 mm above the target. To prepare the Cu(Ti) films, small rectangular Ti plates were mounted on a Cu target. The purities of the Cu target and the Ti plates were 99.99% and 99.9%, respectively. The film thicknesses were measured using TEM and RBS: the typical thickness of the Cu(Ti) alloy films were controlled to approximately 400 nm.

The samples were annealed in ultra high vacuum (UHV) isothermally at 400°C-650°C for 2 h-72 h. The electrical resistivity in the Cu(Ti) films was measured by a four-point probe method. The film microstructures were analyzed by X-ray diffraction (XRD) and TEM. The Ti segregation to the interface was investigated by RBS. Ti segregation only at the interface was observed after the annealing in UHV. For the RBS measurements, $^4He^{2+}$ ion beams with energy of 2 MeV were impinged perpendicularly onto the film surfaces.

## RBS THEORY AND CRITERIA OF FIT

The peak area ($A$) of an element in an RBS profile is the product of the incident beam dose ($Q$), the number of the element atoms in a unit of area ($N$), the scattering cross section of the element atom ($\sigma$), and the solid angle of the detector ($\Omega$):[4]

$$A = QN\sigma\Omega . \quad (1)$$

The molar amount of Ti atoms segregated to the interface ($n$) was estimated by dividing

the number ($N$) from eq. (1), above, by Avogadro's number $N_A$:

$$n = N/N_A = A/N_A Q\sigma\Omega\,. \qquad (2)$$

In the present study, each Ti peak was fitted by a Gaussian curve and an error function, and the $A$ value was determined from the area under the fitted curve. The values of $Q$, $\Omega$, and $\sigma$ of Ti atoms were $3.12 \times 10^{13}$ (10 μC), $3 \times 10^{-3}$ (steradian), and $6.28 \times 10^{-29}$ $m^2$ (0.628 barn), respectively.

To obtain the $A$ values originating in the Ti atoms segregated at the interface, the observed RBS intensities around the Ti peaks in the RBS profiles were fitted by the sum of three components: Ti segregation at the interface, Ti atoms in the alloy film, and a Cu edge above the Ti segregation at the interface (Fig. 2). The RBS profiles were adjusted through refinement of the parameters until the residual, $w_i(y_i(\text{obs})- y_i(\text{calc}))^2$, was minimized in some sense, where $w_i = 1/y_i(\text{obs})$, $y_i(\text{obs})$ = observed intensity at the i-th step, and $y_i(\text{calc})$ = calculated intensity at the i-th step. A best fit of the calculated pattern to the observed pattern was obtained on the basis of various indicators. One of the important indicators is the weighted pattern $R$ index ($R_{wp}$), defined as

$$R_{wp} = \{\sum w_i(y_i(\text{obs})- y_i(\text{calc}))^2/\sum(w_i(y_i(\text{obs}))^2\}^{1/2}. \qquad (3)$$

The numerator of the expression inside the braces is the sum of squared residuals and thus has expected value $o$-$p$, where $o$ and $p$ are the number of observations and the number of parameters, respectively. The expected $R$ index, $R_e$ (another important indicator), is accordingly defined as

$$R_e = \{o\text{-}p/\sum(w_i(y_i(\text{obs}))^2\}^{1/2}. \qquad (4)$$

The ratio $R_{wp}/R_e$ ($=S$) is a measure of how well the fitted model accounts for the data.[5] For example, an $S$ value of 1.3 or less is usually considered to be quite satisfactory, whereas an $S$ value of 1.7, on the other hand, is a probable warning that we should look further into

the reasons and question the adequacy of our model.

## RESULTS AND DISCUSSION

### RBS Measurements and Refinement of Fit in the Cu(Ti)/Low-k1 Samples

Figure 1 shows RBS profiles of Cu(Ti)/low-k1 samples after annealing in UHV. For comparison, those before annealing are shown in Figures 1(b), 1(d), and 1(f). Ti peaks were observed only at the interfaces in all the samples. The Ti-peak intensities increased with increasing annealing time (Figs. 1(a), 1(c), and 1(e)) and annealing temperature (Figs. 1(b), 1(d), and 1(f)). Similar RBS profiles were obtained in all the samples after annealing in UHV prepared on other dielectric-layers (not shown here).

Figure 2 shows portions (around the Ti peaks) of the RBS profiles of Cu(Ti)/low-k1 samples after annealing at 400°C for 2 h in UHV (Fig. 1), and refinement plots (solid line) were placed upon the observed data. The refinement plots consisted of three components: Ti segregation at the interface, Ti atoms in the alloy film, and a Cu edge above the Ti segregation at the interface. The *S* values were in the range of 1.0 to 1.3 in all the samples, with initial Ti concentrations of 1 at.%, 5 at.%, and 10 at.%, which were low enough to indicate an adequate model. The high $R_{wp}$ value in the sample with initial Ti concentrations of 1 at.% was probably due to small reaction of the Ti atoms with the low-k1 layer (a low Ti peak) and considerable overlap between component plots originating in the Ti segregation at the interfaces and Ti atoms in the alloy film. The small $R_{wp}$ values in the other two samples are attributed to large reaction of the Ti atoms with the low-k1 layers.

Similarly, the RBS refinement processes were conducted in the Cu(Ti)/low-k1 samples annealed at other annealing temperatures and times, and the *A* values originating

in the Ti atoms segregated at the interface were obtained. Also, a portion of the RBS profiles around the Ti peaks at the interface in the Cu(Ti)/dielectric-layer samples after annealing in UHV were similarly fitted. The *n* values estimated from the obtained *A* values originating in the Ti atoms segregated at the interface (eq. (2)) are summarized in later sections.

**Comparison of Growth Analyses Using RBS, TEM and Resistivity Results**

Growth of the Ti-rich interface layers on the dielectric layers after the annealing is exhibited as *n* values estimated from the *A* values originating in the Ti atoms segregated at the interface. Plots of *n* vs annealing time (*t*) for Cu(1 at.%Ti)/dielectric-layer samples are shown in Figure 3(a). For comparison, annealing-time dependence on the thickness of the Ti-rich interface layers obtained by TEM and that of the resistivity difference between as-deposited and annealed samples are shown in Figures 3(b)[3] and 3(c), respectively. The *n* values, the thicknesses of the Ti-rich interface layers, and the resistivity differences increased with increasing annealing time and arrived at saturating values. The resistivity decrease in the annealed samples was attributed partly to decrease in impurity scattering The annealing-time dependence in the three figures was similar. All three values in the annealed samples prepared on low-k1 were the largest, followed by those on SiCO or SiCN, while that on $SiO_2$ was the smallest in all the figures. These factors indicate that an RBS technique is an appropriate method for investigation of growth of the Ti-rich interface layers formed on these dielectric layers.

**Growth Behavior of the Ti-Rich Interface Layers**

Figures 4(a)-4(c) show the growth behaviors of the Ti-rich interface layers after

annealing at 400°C for the inital Ti concentrations of 1 at.%, 5 at.%, and 10 at.%, respectively. The *n* values increased with increasing annealing time and gradually arrived at saturating values in all the samples. The *n* values for the Cu(1 at.%Ti) samples were lower than those of the Cu(5 at.%Ti) and Cu(10 at.%Ti) samples, which were similar. The Ti concentration in the alloy films continued to decrease during the reaction of the Ti atoms with the dielectric layers. This suggests that the initial Ti concentration of 1 at.% is insufficient to react with the dielectric layers. Growth of the Ti-rich interface layers observed on low-k1 was faster than those observed on SiCO and SiCN at all the initial Ti concentrations, while the growth on $SiO_2$ varied with the initial Ti concentration.

On the other hand, growth behavior of the Ti-rich interface layers was defined by

$$n = Z \cdot \exp(-E/RT) \cdot t^m, \quad (5)$$

where $Z$ is a preexponential factor and $E$ the activation energy for the reaction. The plots of $n$ vs $t$ (Fig. 4) were transformed to plots of log $n$ vs log $t$, and those are shown in Figure 5. The log $n$ values were found to be proportional to the log $t$ values in all the samples, regardless of the initial Ti concentration in the alloy films or the kinds of dielectric layers. The $m$ values were estimated from the slopes of the log $n$-log $t$ lines. They were almost similar for all the samples regardless of the kinds of dielectric layers at each initial Ti concentration in the alloy films. The $m$ value estimated at the initial Ti concentration of 1 at.% was a little higher than those at 5 at.% and 10 at.%, which were the same. The similar $m$ values suggest that growth of the Ti-rich interface layers was controlled by a similar mechanism. The $m$ values were around 0.2, lower than 0.5, suggesting that growth of the Ti-rich interface layers is not controlled by lattice diffusion, but controlled by grain-boundary and/or interface diffusion.

**Activation Energies and Reaction Rates of the Growth of the Ti-Rich Interface Layers**

Arrhenius plots of log $n$ vs $1/T$ in Cu(Ti)/dielectric-layer samples for the inital Ti concentrations of 1 at.%, 5 at.%, and 10 at.% are shown in Figures 6(a)-6(c), respectively. These show a linear relationship, and this suggests that the formation of the Ti-rich interface layers was controlled by a thermally-activated process. Slopes of the log $n$ vs $1/T$ lines at the initial Ti concentration of 1 at.% were a little smaller than those at 5 at.% and 10 at.%, which were similar. This corresponds to the behaviors indicated in Figures 4 and 5. Activation energies, $E$, were estimated from the slopes of the log $n$ vs $1/T$ lines. The $E$ values were plotted as a function of C concentration of the dielectric layers, as shown in Figure 7(a). The $E$ values at the initial Ti concentration of 1 at.% were lower than those at 5 at.%Ti and 10 at.%Ti, which were similar. The initial Ti concentration at 1 at.% is insufficient to induce reaction of the Ti atoms with the dielectric layers, as mentioned earlier, and thus the $E$ values at the initial Ti concentrations of 5 at.% and 10 at.% are concluded to be appropriate activation energies of the formation of the Ti-rich interface layers.

The $E$ values for the samples consisting of dielectric layers containing carbon (except $SiO_2$) tended to decrease with decreasing C concentration (decreasing $k$), and those without carbon ($SiO_2$) were much higher than others. This indicates that the reaction of the Ti atoms in the alloy films with the low-k layers is the easiest thermally-activated process. Also, composition of the dielectric layers is suggested to play an important role in the reaction of the Ti atoms with dielectric layers, and the carbon may be a key element to control the reaction. This is similar to the formation rule of Ti compounds (TiC or TiSi) in the Ti-rich interface layers.[2]

The preexponential factors, $Z$, were estimated from intercepts of the slopes in the log $n$-log $t$ lines (Fig. 5) and log $n$ - $1/T$ lines (Fig. 6). The $Z$ values estimated from two different sets of data were the same at each initial Ti concentration and dielectric layer. Parameters of $m$, $Z$, and $E$ for growth behavior of the Ti-rich interface layers in the Cu(Ti)/dielectric-layer samples after annealing in UHV are listed in Table 2. The $Z$ values for the samples consisting of dielectric layers with carbon (except $SiO_2$) tended to decrease with decreasing C concentration (decreasing $k$), and those without carbon ($SiO_2$) were much higher than others. This is similar to the $E$ behavior as shown in Figure 7(a). The preexponential factor shows the frequency with which the Ti atoms meet elemental reactants in the dielectric layers. The frequency was low in the samples with low-k, and was high in the samples with $SiO_2$. In consequence, coefficients of the reaction rate ($Z \cdot \exp(-E/RT)$) were insensitive to C concentration in the dielectric layers at the initial Ti concentrations of 5 at.% and 10 at.%, while those increased with decreasing C concentration at the initial Ti concentration of 1 at.% (Fig. 7(b)). These factors lead to the conclusion that growth of the Ti-rich interface layers is controlled by chemical reactions of the Ti atoms with the dielectric layers represented by the $Z$ and $E$ values. There are few diffusion processes possible in all the samples, since the $m$ values suggest that it is controlled by grain-boundary and/or interface diffusion. However, the growth is believed to be mainly controlled by the chemical reactions because the $E$ and $Z$ values are significantly sensitive to the dielectric layers and the Ti-rich interface layers were complex structures consisting of fine polycrystalline TiC or TiSi in addition to amorphous Ti oxide matrix. Also, composition of the dielectric layers plays an important role in the reaction, and the carbon may be a key element to control the reaction.

Using the low-k layers reduced both the $Z$ and $E$ values, suggesting that there is

some potential to reduce the annealing temperature without reducing the reaction rate. Figure 8 shows the calculated ratio of $Z \cdot \exp(-E/RT)$ to $Z \cdot \exp(-E/R \cdot 673)$ ($T$=400°C) for the Cu(Ti)/dielectric-layer samples as a function of annealing temperature. The reaction rates of the Cu(Ti)/dielectric-layer samples decreased with decreasing annealing temperature, while the reaction rate was large in the samples with low-k, and was small in the samples with $SiO_2$ in the temperature range of 200°C to 400°C at the initial Ti concentrations of 5 at.% and 10 at.%. The reaction rates of the samples with low-k after annealing at 300°C were almost half of those after annealing at 400°C. Furthermore, reducing the initial Ti concentration in the alloy films can increase the reaction rate due to a decrease in effective activation energy. The reaction rates of the samples with low-k1 and low-k4 after annealing at 200°C were almost 50% and 90% of those after annealing at 400°C, respectively. Thus, combination of the low initial Ti concentration in the alloy films and low-k layers is concluded to contribute to a low temperature fabrication technique to prepare low-resistivity Cu wires with self-formed ultra-thin barrier layers.

## CONCLUSIONS

For systematic investigation of the growth of the Ti-rich interface layers in annealed Cu(Ti)/dielectric-layer samples, the RBS technique was employed. Growth behavior observed in RBS was similar to those observed using TEM and resistivity measurements. Thus, the RBS technique is found to be an appropriate method for the analysis of the growth of Ti-rich interface layers.

In all the Cu(Ti)/dielectric-layer samples after annealing in UHV, Ti peaks were obtained only at the interfaces in the RBS profiles. The $n$ values, estimated from the $A$ values originating in the Ti atoms segregated at the interface, increased with increasing

annealing time and temperature. The log *n* values were found to be proportional to the log *t* values. The slopes were almost similar for all the samples. This suggests that the growth mechanism is similar in each case. The activation energy (*E*) for the reaction of the Ti atoms with the dielectric layers containing carbon (except $SiO_2$) tended to decrease with decreasing C concentration (decreasing *k*), and those without carbon ($SiO_2$) were much higher than others. The preexponential factor (*Z*) values similarly varied with C concentration in the dielectric layers. As a consequence, coefficients of the reaction rate ($Z \cdot \exp(-E/RT)$) were insensitive to C concentration in the dielectric layers at the initial Ti concentrations of 5 at.% and 10 at.%, while those increased with decreasing C concentration at the initial Ti concentration of 1 at.%. These factors lead to the conclusion that growth of the Ti-rich interface layers is controlled by chemical reactions, represented by the *Z* and *E* values, of the Ti atoms with the dielectric layers, although there are a few diffusion processes possible. Also, the composition of the dielectric layers plays an important role in the reaction, and the carbon may be a key element to control the reaction. Using the low-k layers reduced both the *Z* and *E* values, suggesting that there is some potential to reduce annealing temperature without reducing reaction rate.

**ACKNOWLEDGEMENTS**

This work was supported by Research Fellowships of the Japan Society for the Promotion of Science for Young Scientists (Kohama) and Grants-in-Aid for the Global COE Program, “International Center for Integrated Research and Advanced Education in Materials Science,” from the Ministry of Education, Culture, Sports, Science and Technology of Japan.

**REFERENCES**


1. S. Tsukimoto, M. Moriyama, K. Ito, and M. Murakami, J. Electron. Mat., 34, 592-599 (2005).
2. K. Kohama, K. Ito, S. Tsukimoto, K. Mori, K. Maekawa, and M. Murakami, J. Electron. Mat., 37, 1148-1157 (2008).
3. K. Kohama, K. Ito, S. Tsukimoto, K. Mori, K. Maekawa, and M. Murakami, Mater. Trans., 49, 1987-1993 (2008).
4. W.-K. Chu, J.W. Mayer, and M.-A. Nicolet, Backscattering Spectrometry, San Diego : Academic Press, 1978, pp. 91-92.
5. R.A. Young, The Rietveld Method, New York : Oxford University Press, 1993, pp. 22.

Table 1 Dielectric constants, *k*, of the dielectric layers and their C, O, Si, and N concentrations (at.%).

| Dielectric layers | *k* | C (at.%) | O (at.%) | Si (at.%) | N (at.%) |
|---|---|---|---|---|---|
| SiCN | 4.8 | 21.4 | 0.5 | 25.0 | 12.8 |
| SiCO | 4.5 | 20.8 | 16.6 | 24.6 | - |
| low-k1 | 3.0 | 17.0 | 24.9 | 18.8 | - |
| low-k4 | 2.6 | ~14 | ~29 | ~18 | - |
| $SiO_2$ | 3.9 | - | 66.7 | 33.3 | - |

Table 2 Parameters for growth behavior of the Ti-rich interface layers in the Cu(Ti)/dielectric-layer samples after annealing in UHV: *m* values, preexponential factors, *Z*, and activation energies, *E*.

| Dielectric layers | Initial Ti contents in Cu(Ti) alloy films (at.%) | m | Z ($mol/m^2/h^m$) | E (kJ/mol) |
|---|---|---|---|---|
| SiCN | 1 | 0.192 | 0.00226 | 13.6 |
| | 5 | 0.137 | 1.48 | 44.9 |
| | 10 | 0.177 | 26.1 | 60.4 |
| SiCO | 1 | 0.223 | 0.00258 | 16.2 |
| | 5 | 0.176 | 0.882 | 43.1 |
| | 10 | 0.148 | 0.929 | 42.0 |
| low-k1 | 1 | 0.223 | 0.00115 | 9.70 |
| | 5 | 0.125 | 0.0457 | 25.2 |
| | 10 | 0.146 | 0.0173 | 17.4 |
| low-k4 | 1 | 0.220 | 0.000361 | 1.29 |
| | 5 | 0.150 | 0.0390 | 24.4 |
| | 10 | 0.150 | 0.0749 | 29.4 |
| $SiO_2$ | 1 | 0.224 | 0.122 | 42.8 |
| | 5 | 0.124 | 87.4 | 81.3 |
| | 10 | 0.168 | 31.3 | 74.4 |

Figure captions

Fig. 1 RBS profiles of the Cu(Ti)/low-k1 samples after annealing in UHV at 400°C for various annealing times ((a), (c), and (e)) and after annealing in UHV at various annealing temperatures ((b), (d), and (f)) for 2 h. The initial Ti concentrations are (a) and (b) 1 at.%, (c) and (d) 5 at.%, and (e) and (f) 10 at.%. For comparison, RBS profiles before annealing are plotted in Figures (b), (d), and (f).

Fig. 2 Portions (around the Ti peaks) of the RBS profiles of Cu(Ti)/low-k1 samples after annealing at 400°C for 2 h in UHV (Fig. 1) and refinement plots (solid line) placed upon the observed data. The refinement plots consisted of three components: Ti segregation at the interface, Ti atoms in the alloy film, and a Cu edge above the Ti segregation at the interface. The initial Ti concentrations are (a) 1 at.%, (b) 5 at.%, and (c) 10 at.%.

Fig. 3 (a) Plots of $n$ vs annealing time ($t$) for Cu(1 at.%Ti)/dielectric-layer samples after annealing at 400°C in UHV. For comparison, (b) annealing-time dependence of the thicknesses of the Ti-rich interface layers obtained by TEM and (c) that of the resistivity difference between as-deposited and annealed samples.

Fig. 4 Plots of $n$ vs $t$ for Cu(Ti)/dielectric-layer samples after annealing at 400°C in UHV. The initial Ti concentrations are (a) 1 at.%, (b) 5 at.%, and (c) 10 at.%.

Fig. 5 Plots of log $n$ vs log $t$ for Cu(Ti)/dielectric-layer samples after annealing at 400°C in UHV. The initial Ti concentrations are (a) 1 at.%, (b) 5 at.%, and (c) 10 at.%.

Fig. 6 Arrhenius plots of log $n$ vs $1/T$ for Cu(Ti)/dielectric-layer samples after annealing for 2 h in UHV. The initial Ti concentrations are (a) 1 at.%, (b) 5 at.%, and (c) 10 at.%.

Fig. 7 (a) Activation energies of $E$ and (b) values of $Z \cdot \exp(-E/RT)$ of the Cu(Ti)/dielectric-layer samples after annealing in UHV, as a function of C concentration of the dielectric layers.

Fig. 8 The ratio of $Z \cdot \exp(-E/RT)$ to $Z \cdot \exp(-E/R \cdot 673)$ (T=400°C) for the Cu(Ti)/dielectric-layer samples as a function of annealing temperature. The initial Ti concentrations are (a) 1 at.%, (b) 5 at.%, and (c) 10 at.%.

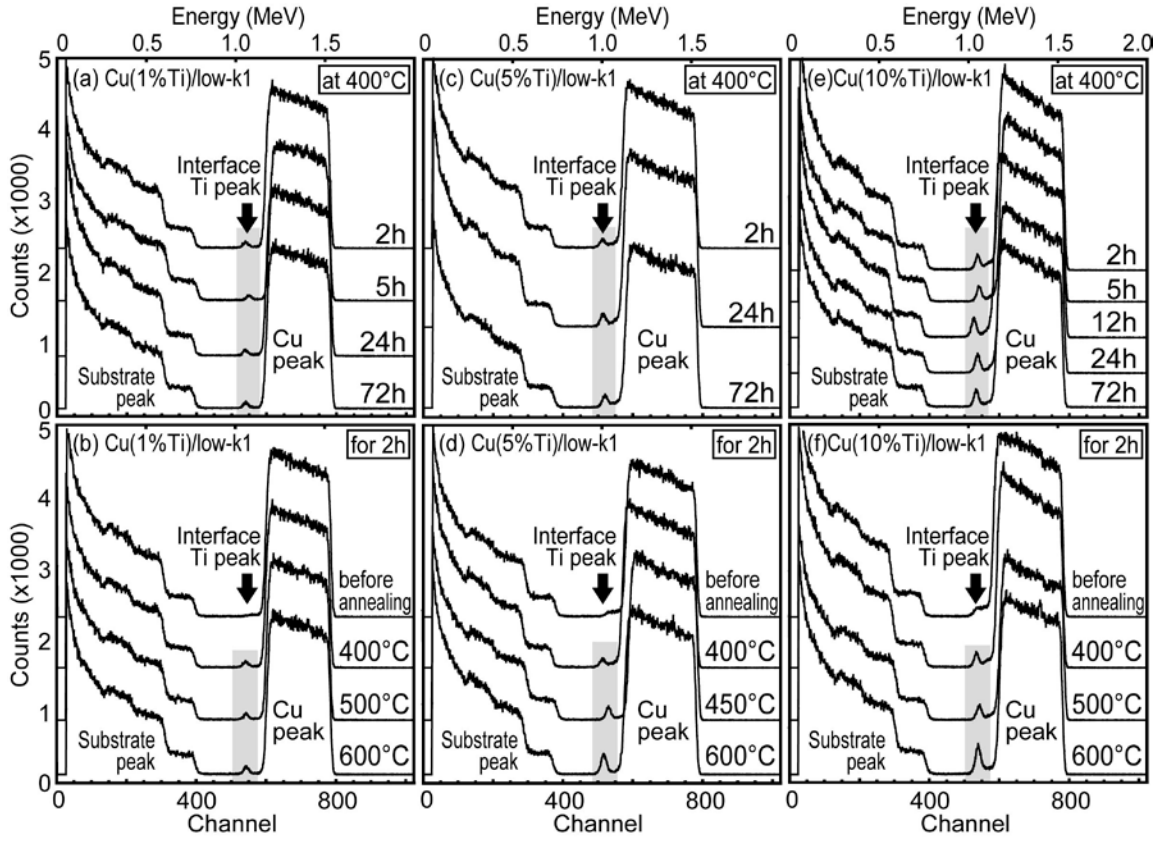
Energy (MeV)
(a) Cu(1%Ti)/low-k1
at 400°C
(c) Cu(5%Ti)/low-k1
(e)Cu(10%Ti)/low-k1
Interface Ti peak
Cu peak
Substrate peak
2h
5h
12h
24h
72h
(b) Cu(1%Ti)/low-k1
for 2h
(d) Cu(5%Ti)/low-k1
(f)Cu(10%Ti)/low-k1
before annealing
400°C
450°C
500°C
600°C
Counts (x1000)
Channel

Fig. 1

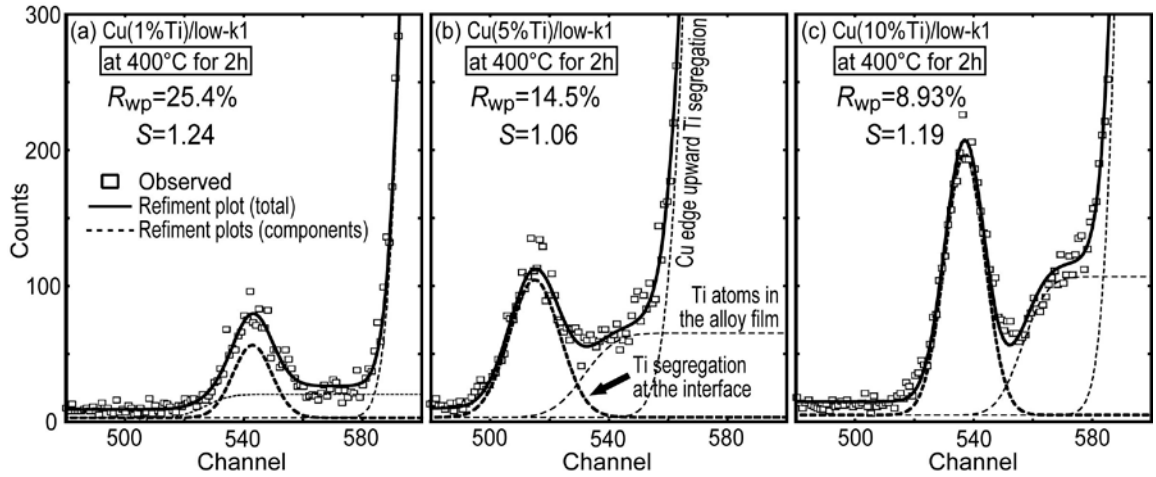
(a) Cu(1%Ti)/low-k1
at 400°C for 2h
$R_{wp}$=25.4%
$S$=1.24
Observed
Refiment plot (total)
Refiment plots (components)
(b) Cu(5%Ti)/low-k1
$R_{wp}$=14.5%
$S$=1.06
Cu edge upward Ti segregation
Ti atoms in the alloy film
Ti segregation at the interface
(c) Cu(10%Ti)/low-k1
$R_{wp}$=8.93%
$S$=1.19
Counts
Channel

Fig. 2

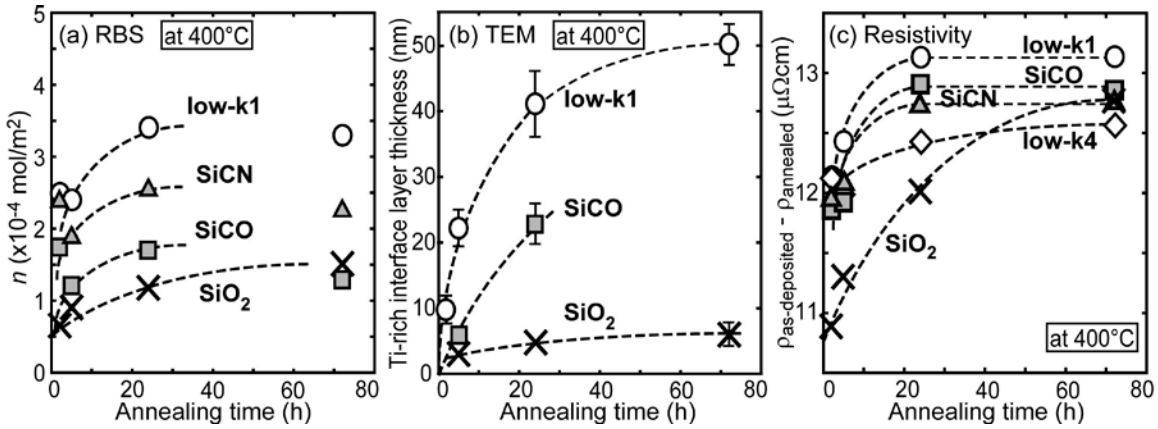
(a) RBS at 400°C
low-k1
SiCN
SiCO
SiO2
n (x10-4 mol/m2)
Annealing time (h)
(b) TEM at 400°C
low-k1
SiCO
SiO2
Ti-rich interface layer thickness (nm)
Annealing time (h)
(c) Resistivity
low-k1
SiCO
SiCN
low-k4
SiO2
at 400°C
ρas-deposited - ρannealed (μΩcm)
Annealing time (h)

Fig. 3

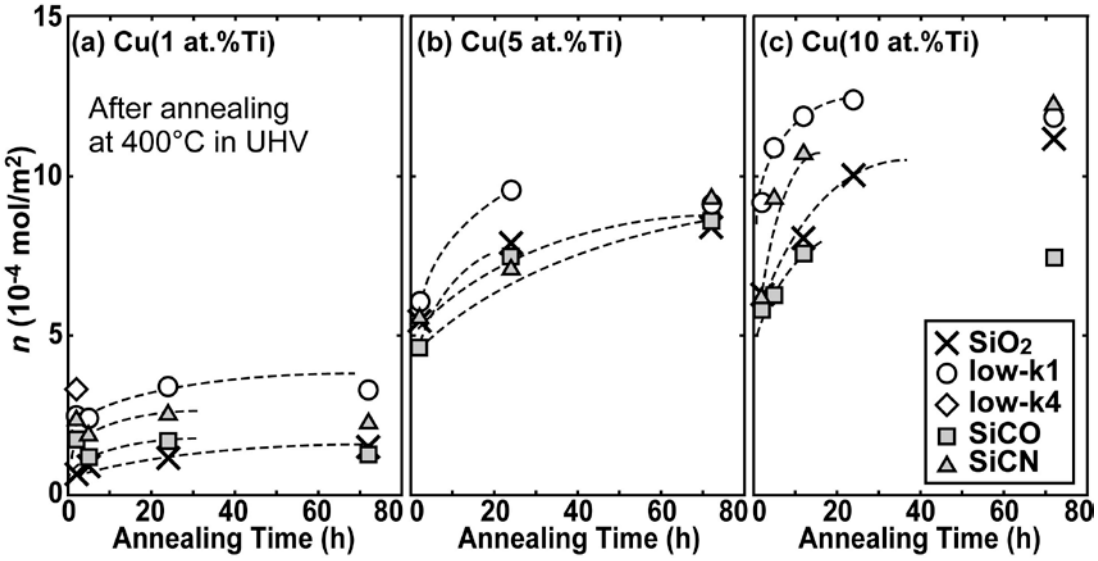
(a) Cu(1 at.%Ti)
After annealing
at 400°C in UHV
(b) Cu(5 at.%Ti)
(c) Cu(10 at.%Ti)
n (10-4 mol/m2)
Annealing Time (h)
Annealing Time (h)
Annealing Time (h)
SiO2
low-k1
low-k4
SiCO
SiCN

Fig. 4

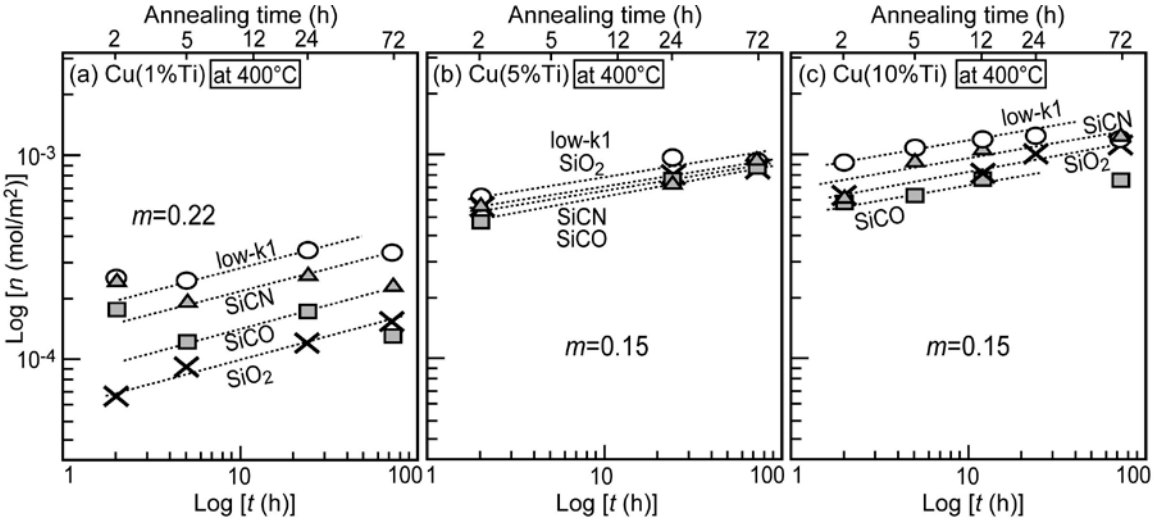
Annealing time (h)
2 5 12 24 72
(a) Cu(1%Ti) at 400°C
(b) Cu(5%Ti) at 400°C
(c) Cu(10%Ti) at 400°C
Log [n (mol/m²)]
10-3
10-4
m=0.22
m=0.15
m=0.15
low-k1
SiCN
SiCO
SiO2
1 10 100
Log [t (h)]

Fig. 5

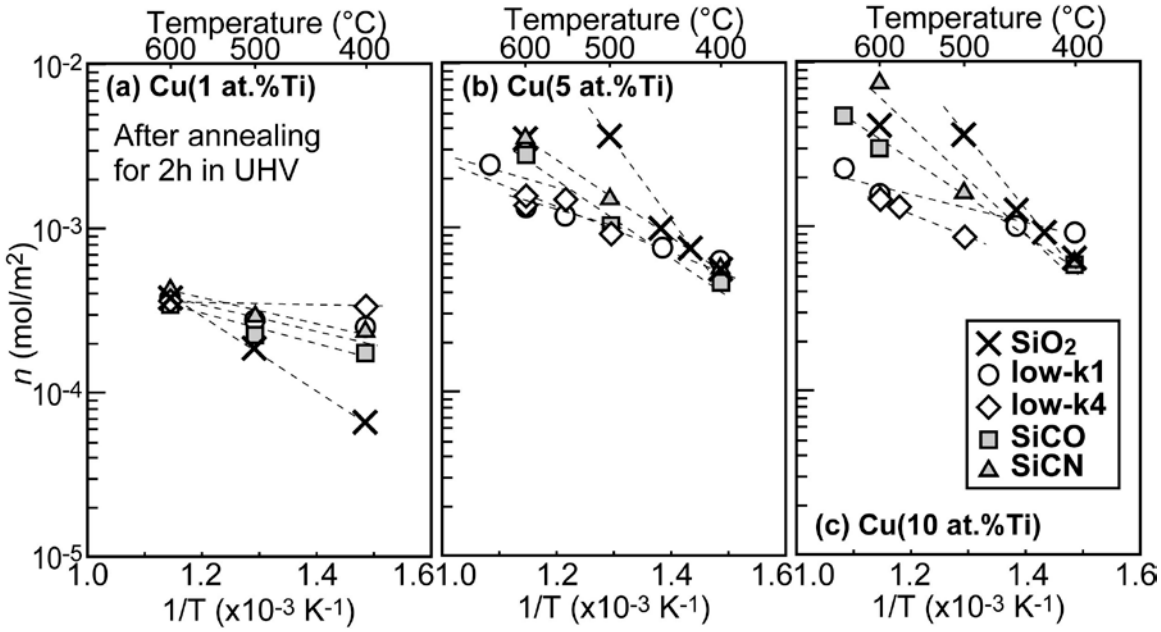
Temperature (°C)
600 500 400
(a) Cu(1 at.%Ti)
After annealing
for 2h in UHV
(b) Cu(5 at.%Ti)
(c) Cu(10 at.%Ti)
n (mol/m²)
10-2
10-3
10-4
10-5
1.0 1.2 1.4 1.6
1/T (x10-3 K-1)
SiO2
low-k1
low-k4
SiCO
SiCN

Fig. 6

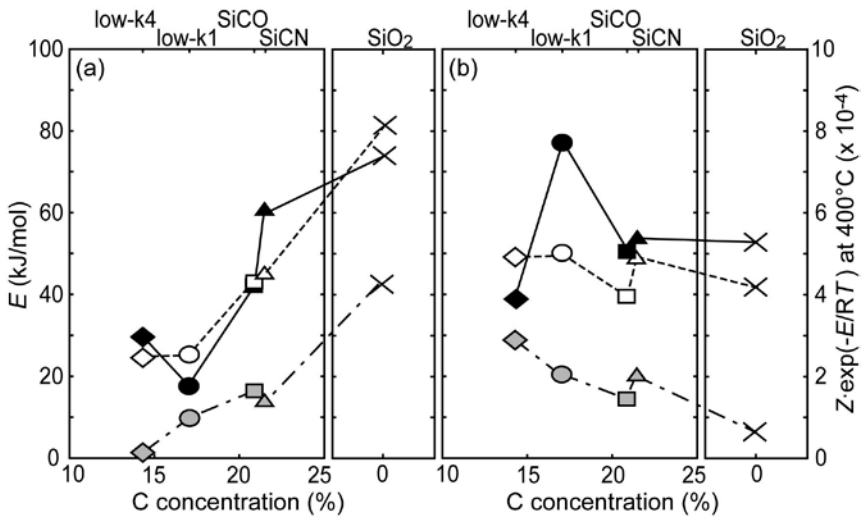
low-k4
SiCO
low-k1
SiCN
SiO2
(a)
(b)
E (kJ/mol)
Z·exp(-E/RT) at 400°C (x 10-4)
C concentration (%)
C concentration (%)

Fig. 7

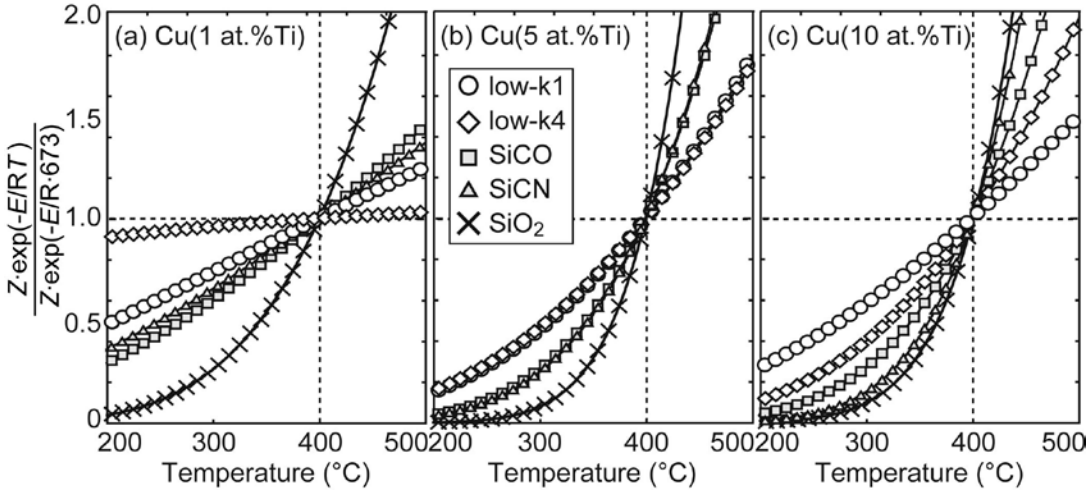
(a) Cu(1 at.%Ti)
(b) Cu(5 at.%Ti)
(c) Cu(10 at.%Ti)
low-k1
low-k4
SiCO
SiCN
SiO2
Z·exp(-E/RT) / Z·exp(-E/R·673)
Temperature (°C)
Temperature (°C)
Temperature (°C)

Fig. 8